論文 / 著書情報
Article / Book Information

題目(和文)	結晶性-結晶性 2 元ブ　ロック共重合体の同時結晶化挙動
Title(English)	Simultaneous Crystallization Behavior of Crystalline－crystalline Diblock Copolymers
著者(和文)	大澤俊
Author(English)	Satoshi Osawa
出典(和文)	学位:博士(工学), 学位授与機関:東京工業大学, 報告番号:甲第11088号, 授与年月日:2019年3月26日, 学位の種別:課程博士, 審査員:野島 修一,扇澤 敏明,中嶋 健,川内 進,古屋 秀峰
Citation(English)	Degree:Doctor (Engineering), Conferring organization: Tokyo Institute of Technology, Report number:甲第11088号, Conferred date:2019/3/26, Degree Type:Course doctor, Examiner:,,,,
学位種別(和文)	博士論文
Category(English)	Doctoral Thesis
種別(和文)	要約
Type(English)	Outline

論 文 要 約

Simultaneous Crystallization Behavior of Crystalline−crystalline Diblock Copolymers

（結晶性-結晶性２元ブロック共重合体の同時結晶化挙動）

有機・高分子物質 専攻　　大澤 俊

In this study, various polyethylene-*block*-poly(*β*-propiolactone) (PE-*b*-PPL) diblock copolymers are synthesized and the mechanism of simultaneous crystallization in crystalline-crystalline diblock copolymers is investigated. The PE-*b*-PPL has unique and appropriate characteristics for this purpose, that is, both blocks have close crystallizable temperatures T_c and show a strong segregation behavior, where the microdomain structure is preserved after the crystallization of both blocks. Furthermore, the electron densities of PE and PPL are quite different, so that it is possible to examine a detailed morphology after crystallization using small-angle X-ray scattering (SAXS) techniques.

In **Chapter 1,** the introduction and the purpose of this study were described.

In **Chapter 2**, the synthesis method employed in this study and the molecular characteristics of PE-*b*-PPL used in Chapters 3-5 were described in detail.

In **Chapter 3**, the crystallization behavior of PE-*b*-PPL copolymers was systematically examined with a wide range of crystallinity of PE blocks X_{PE} ($0 \leq X_{PE} \leq 0.33$) to clarify the simultaneous crystallization of PE-*b*-PPL. X_{PE} was controlled by changing the proportion of ethyl branches in PE blocks ($\psi_{1\text{-}2}$). Based on the results of DSC experiments for PE-PL*x* (*x* stands for the value of $\psi_{1\text{-}2}$, where x = 5, 6, 10, 15, 20, or 31), the melting temperature of PE blocks decreased linearly with decreasing X_{PE}, whereas that of PPL blocks was independent of X_{PE}. These experimental results indicate that the lamella thickness of PE blocks is largely affected by X_{PE} and that the lamella thickness of PPL blocks is constant against the crystallizability of PE blocks.

Next, the morphology of PE-*b*-PPL copolymers before and after crystallization was examined by SAXS with synchrotron radiation (SR-SAXS). It was revealed that both PE and PPL blocks were strongly segregated to form some microdomain structure in the melt. On the other hand, the

morphology after crystallization was quite different from that in the melt and it depended significantly on $\psi_{1\text{-}2}$. For example, in PE-PL6 (X_{PE} = 0.32), the lamellar microdomain structure was completely destroyed and replaced with crystalline lamellar morphology. On the other hands, in PE-PL10, PE-PL15, and PE-PL20 (X_{PE} = 0.12-0.26), the PE blocks rapidly crystallized in the lamellar microdomain structure and enhanced the stability of this morphology against the subsequent crystallization of PPL blocks. In PE-PL31 (X_{PE} = 0), the PE blocks did not crystallize and only PPL blocks crystallized from the lamellar microdomain structure.

The crystallization behavior of PE-*b*-PPL was further examined using time-resolved SR-SAXS and Fourier transform infra-red spectroscopy (FTIR). As for PE-PL6, the long period L increased rapidly at the early stage of crystallization due to the advance crystallization of PE blocks, then L increased slightly at the middle stage of crystallization due to the crystallization of PPL blocks. This indicates that the lamellar microdomain structure in the melt is completely destroyed due to the strong crystallizability of PE blocks and that the crystalline lamellar morphology consisting of both crystallized PE and PPL blocks is formed by a two-step crystallization. As for PE-PL10, L remained almost constant during the crystallization, suggesting that the crystallization of PE blocks proceeded within the lamellar microdomain structure formed in the melt due to relatively low crystallizability. The PPL blocks subsequently crystallized in the PE crystalline microdomain structure, which was reinforced and stabilized against the crystallization of PPL blocks due to the advance crystallization of PE blocks. Consequently, the crystalline lamellar microdomain structure consisting of crystallized PE and PPL blocks yielded in the system. For PE-PL31, the PE blocks did not crystallize due to low crystallizability of PE blocks and L changed significantly with the crystallization of PPL blocks, suggesting a break-out crystallization from a lamellar microdomain structure into a crystalline lamellar morphology.

Based on the results obtained in this chapter, the morphology formation observed in PE-*b*-PPL copolymers is classified into following three types by the value of X_{PE} (**Figure 6.1**).

1. X_{PE} (> 0.3) (PE-PL5 and PE-PL6)

The lamellar microdomain structure formed in the melt is completely destroyed by the advance crystallization of PE blocks and the crystalline lamellar morphology is formed instead. PPL blocks subsequently crystallize within the PE crystalline lamellar morphology to yield crystalline lamellar morphology (upper route in **Figure 6.1**).

2. 0.12 < X_{PE} < 0.26 (PE-PL10, PE-PL15, and PE-PL20)

The crystallizability of PE blocks is not large enough not to destroy the lamellar microdomain structure, and PE blocks crystallize within it. The crystallization of PE blocks reinforces and stabilizes the existing lamellar microdomain structure against the subsequent crystallization of

PPL blocks. The PPL blocks also do not destroy the lamellar microdomain structure and crystallize within it (middle route in **Figure 6.1**).

3. $X_{PE} = 0$ (PE-PL31)

Only PPL blocks crystallize to form crystalline lamellar morphology. This morphological transition occurs when the PE blocks do not crystallize and the lamellar microdomain structure is not reinforced (lower route in **Figure 6.1**).

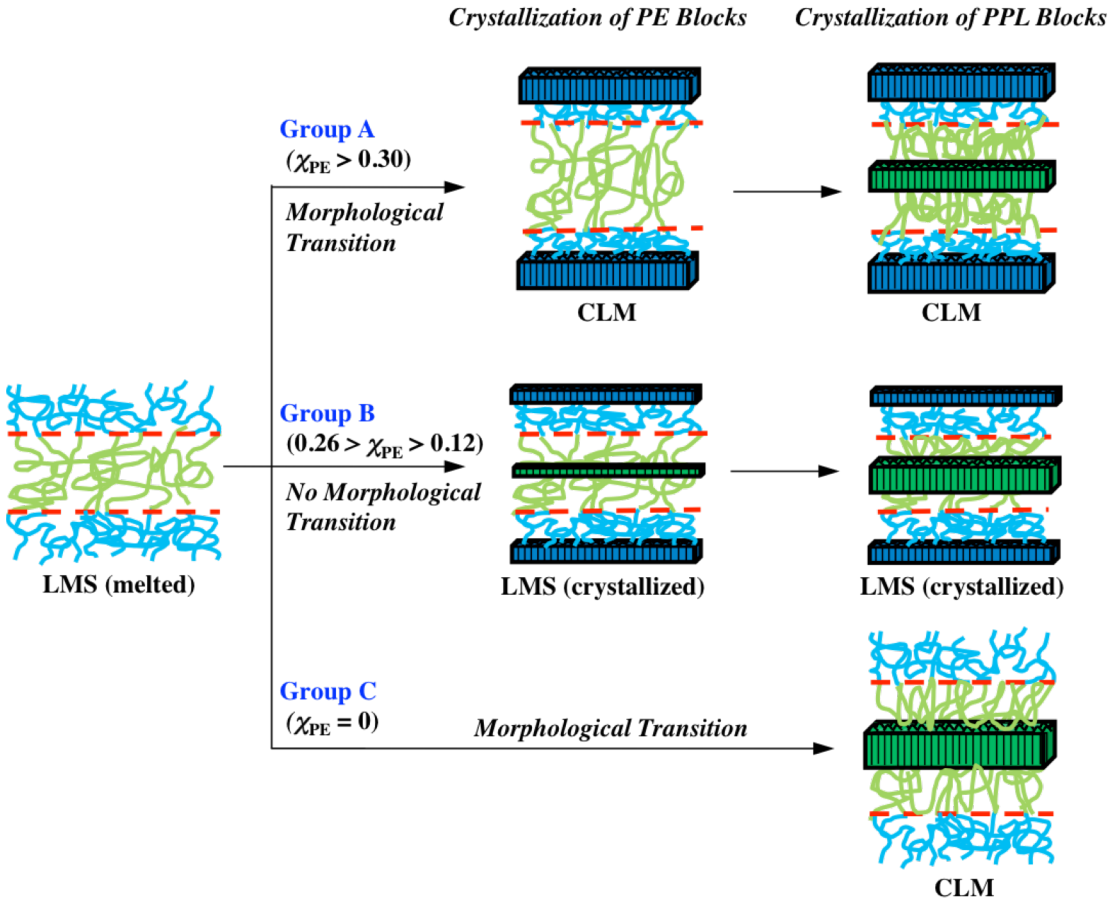

Figure 6.1 Schematic illustration showing the morphology formation in the crystallization of PE-*b*-PPL copolymers, which is usefully divided into three groups (group A, group B, and group C) depending on X_{PE}. LMS and CLM are short for lamellar microdomain structure and crystalline lamellar morphology, respectively.

In **Chapter 4**, we crystallized PPL blocks separately into the β-form (βPPL) or δ-form (δPPL), and investigated the effects of crystal structures of PPL blocks on the crystallization behavior of PE-*b*-PPL. This is the first study to achieve different crystalline morphologies by using the polymorphism of constituent blocks in crystalline-crystalline diblock copolymers. To make T_c of PE

and PPL blocks closer, PE blocks with $\psi_{1\text{-}2}$ = 18% were used. We first characterized the synthesized PE-*b*-PPL using FTIR and SR-WAXD. It was revealed that the sample annealed at 45 °C consisted of a mixture of PPLδ and PPLβ with the molar ratio of δ:β = 80:20 along with the modest amounts of PE crystals (EPLδ). Meanwhile, the sample annealed at 130 °C consisted of PPL crystals with only PPLβ and modest amounts of PE crystals (EPLβ).

Next, we examined the morphologies of EPLβ and EPLδ in the melt and after crystallization by SR-SAXS. It was revealed that EPLδ and EPLβ in the melt formed lamellar microdomain structures with a sharp interface. After crystallization, the lamellar microdomain structure formed in the melt was practically preserved, although the regularity was extremely decreased.

The lamellar microdomain structures were further evaluated quantitatively by fitting the SR-SAXS curves with theoretical ones. The regularity of each layer (σ/L) showed that lamellar microdomain structures in the melt were well ordered. The value of σ/L of EPLδ (0.364) was significantly larger than that of EPLβ (0.179) after crystallization, indicating that the large distortion of lamellar microdomain structures was caused by the crystallization of δPPL. To understand the difference in the crystallization mechanism between EPLδ and EPLβ, time-resolved simultaneous SR-SAXS/WAXD was performed. The values of L and FWHM of the first peak in both EPLδ and EPLβ slightly increased at the early stage of crystallization. This clearly indicated that the crystallization of EPLδ and EPLβ did not take the morphological transition from a lamellar microdomain structure into a crystalline lamellar morphology. In particular, it was found that δPPL and PE crystallized cooperatively and/or interactively in EPLδ. The simultaneous crystallization of PE and δPPL blocks would control the morphology formation in crystalline EPLδ. As for EPLβ, only PE blocks crystallized at the beginning of the crystallization of EPLβ, and then βPPL crystallized after complete crystallization of PE blocks. Therefore, the difference in the final crystalline morphology formed in EPLδ and EPLβ was mainly ascribed to the difference in the crystallization mechanism between δPPL and βPPL blocks. In summary, we propose the crystallization mechanism of EPLδ and EPLβ based on the results obtained in this chapter (**Figure 6.2**).

EPLδ

The δPPL blocks crystallized simultaneously with PE blocks, which led to the combined crystallization and the large crystallinity, yielding the largely distorted lamellar microdomain structure (upper route in **Figure 6.2**).

EPLβ

The sequential crystallization of PE and βPPL blocks in EPLβ did not destroy the lamellar microdomain structure, because the crystallizability of PE blocks was sufficiently small. The PE

blocks crystallized within the lamellar microdomain structure and stabilized it against the subsequent crystallization of βPPL blocks. As a result, the advance crystallization of PE blocks slightly deformed the lamellar microdomain structure, and the sequential crystallization of βPPL blocks occurred within the crystallized lamellar microdomain structure (lower route in **Figure 6.2**).

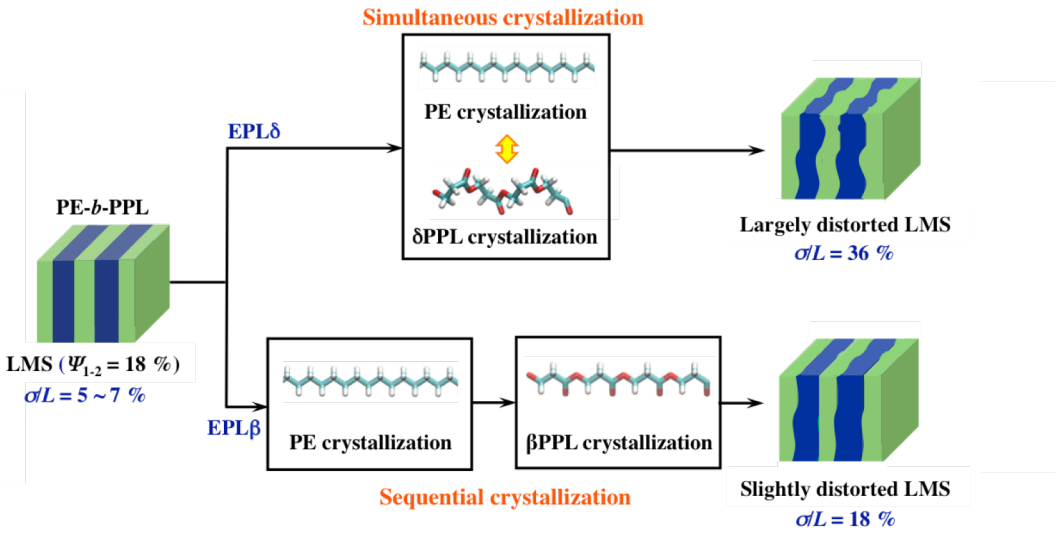

Figure 6.2 Schematic illustration showing the difference in morphology formation between EPLδ and EPLβ. The difference in the crysallized morphology arises from the crystallization mechanism of δPPL and βPPL blocks. L : the alternating distance of the morphology, σ : the standard deviation of L, σ/L : a measure for the degree of distortion of the morphology.

In **Chapter 5**, we examined the simultaneous crystallization of PE-*b*-PPL when the PE blocks were confined in a cylindrical microdomain structure to decrease T_c of PE blocks to the extent comparable to that of PPL blocks. This method has an advantage for using chemically "pure" PE blocks without decreasing the crystallizability due to high $\psi_{1\text{-}2}$. The value of $\psi_{1\text{-}2}$ = 10% was used in this study, which was the same as that obtained by usual anionic polymerization. To form a cylindrical microdomain structure, the volume fraction of PE blocks in PE-*b*-PPL φ_{PE} was controlled to be about 0.3 by changing the molecular weight of PE and PPL blocks. Furthermore, in this chapter, PE-*b*-PPL copolymers with PPL blocks crystallized into β-form (EPLβ) or δ-form (EPLδ) were separately prepared by controlling the thermal history.

Although the results of DSC measurements were complicated, the cylindrical microdomain structures of EPLβ and EPLδ in the melt were confirmed by SR-SAXS results. It was also revealed that the morphologies of EPLβ and EPLδ were practically preserved through the crystallization (i.e.

break-out crystallization did not occur), however, the regularity was decreased after crystallization. The long period of microdomain structures L and full width at half maximum (FWHM) of the first peak in the SR-SAXS curves were examined by time-resolved SR-SAXS experiments. The L and FWHM values of EPLδ during crystallization were monotonically increased, as the crystallinities of PE and δPPL blocks. The discontinuous change in L and FWHM was not observed during the crystallization of EPLδ. Therefore, simultaneous crystallization with PE blocks confined in cylindrical nanodomains successfully achieved during the isothermal crystallization of EPLδ without using PE blocks having higher $\psi_{1\text{-}2}$ values.

Finally, the general conclusion of the simultaneous crystallization of crystalline -crystalline diblock copolymers is described in **Chapter 6.**

The synthesis of macromolecules having new properties and functions has been drawing much attention. Controlling the nanoscale structure of component materials has been intensively studied in order to achieve this purpose. Crystalline-crystalline diblock copolymers are an interesting and promising system to develop new properties and functions, because they have two kinds of crystallization process interacting with each other. Furthermore, their crystallization process is complicated and the difference of melting temperatures, morphologies, and segregation forces of both components affects the crystallization mechanism.

In this study, we especially focused on PE-*b*-PPL diblock copolymers. We synthesized them, controlled the crystal structure of PPL blocks, and examined the effects of this crystal structure on the morphology of diblock copolymers after crystallization. As a result, the morphology after crystallization depended remarkably on the crystal structure of PPL blocks. We first achieved the different crystalline morphologies by using the polymorphism of constituent blocks and proposed the mechanism of the crystallization process (Chapter 4).

We also developed the method to control the crystallization rate of component blocks and examined the simultaneous crystallization. We found that the simultaneous crystallization was achieved when the components were confined in a cylindrical microdomain structure without changing the ratio of ethyl branches in PE (Chapter 5). This confinement method would be applied to the synthesis of other crystalline-crystalline diblock copolymers and is promising to pave the way for a new synthetic method by controlling the crystallization rate of component materials.